Spontaneous Fission Spectrum of Neutrons from ^{252}Cf with Kinetic Energies Less than 1 MeV

Suraj Bastola

A senior thesis submitted to the faculty of

Brigham Young University
in partial fulfillment of the requirements for the degree of

Bachelor of Science

Dr. Lawrence Rees, Advisor

Department of Physics and Astronomy

Brigham Young University

August 2012

ABSTRACT

Spontaneous Fission Spectrum of Neutrons from ^{252}Cf
with Kinetic Energies Less than 1 MeV

Suraj Bastola
Department of Physics and Astronomy
Bachelor of Science

The fission spectrum of neutrons plays a significant role in the construction of nuclear reactors. However, the fission spectrum of neutrons with kinetic energies less than 1 MeV, emitted from the spontaneous fission of ^{252}Cf, is not as precisely known as that for higher energy neutrons. A method for making improved measurements of low-energy cross sections is described and results of preliminary tests are reported.

Parts of this work were funded by NNSA Grant no. DE-FG52-10NA29655 and DHS Award no. 2010-DN-077-ARI039-02.

Contents

List of Figures

1 Introduction

Nuclei in which the number of neutrons is considerably larger than the number of protons are unstable and tend to break into daughter nuclei, with concurrent production of neutrons and gammas. This process of breaking of heavy nuclei into smaller fragments is called fission. Nuclear fission, however, can occur in two different modes.

1.1 Stimulated Fission

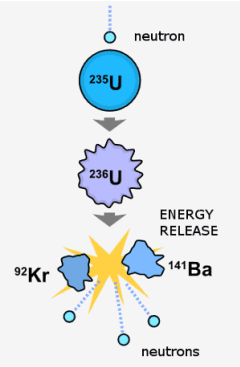

Figure 1: [1]Fission chain reaction in ^{235}U nuclei

If a neutron is absorbed by a heavy nucleus, several MeV of binding energy is released. The heavy nucleus can become unstable and break into fission fragments. This type of fission initiated by neutrons is called stimulated fission.

For example, when a ^{235}U nucleus absorbs a neutron, it splits into barium and krypton, producing neutrons and releasing energy. This is an example of stimulated fission. These neutrons emitted in the fission can be absorbed by other ^{235}U atoms, initiating a chain reaction and releasing huge amount of energy. This stimulated fission is the basis of operation of nuclear reactors.

1.2 Spontaneous Fission

Fission which does not require initiation by another particle is known as spontaneous fission. This is the mode by which ^{252}Cf nucleus undergoes fission. The half life of ^{252}Cf is 2.645 years. Being a very strong neutron emitter, it extremely radioactive and harmful.

^{252}Cf undergoes alpha decay 97% of the time to form ^{248}Cm, and undergoes spontaneous fission remaining 3% of the time. One microgram of ^{252}Cf produces 2.3 million neutrons per second, an average of 3.7 neutrons per spontaneous fission.When ^{252}Cf undergoes spontaneous fission, it produces ^{140}Xe, ^{108}Ru, neutrons and gammas. Approximately, four gammas are produced per neutron during its spontaneous fission. These neutrons produced by ^{252}Cf have different energies. The energy distribution of these fission neutrons, as shown in Fig. 2, is known as the spontaneous fission spectrum.

The spontaneous fission spectrum of neutrons, from 0.003 MeV to 15 MeV, was measured by J.W. Meadows in Argonne National Laboratory around 1965. The primary purpose of this experiment was to measure the lower energy portion of the spectrum. He had employed time-of-flight techniques to measure the lower energy portion of the spectrum. However, the uncertainties in the lower energy part of the measured spectrum were greater than that in the higher energy portion.

[1]Sources to the figures are cited in the Bibliography section.

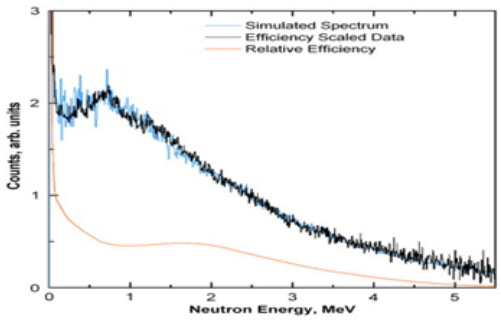

Figure 2: Spontaneous Fission Spectrum of Neutrons from ^{252}Cf

The fission spectrum of neutrons plays a significant role in the construction of nuclear reactors. However, as depicted in Fig. 2, the fission spectrum below 1 MeV is not as precisely known as that for higher energy neutrons. The purpose of this experiment is to measure the fission spectrum below 1 MeV to a greater precision than before.

A Time to Pulse Height Converter (TPHC) was used in Meadows experiment in 1965. However, in his experiment, the output pulses from TPHC were fed to the traditional 512 RCL Channel Analyzer. So, the TPHC pulses have never ever been digitized to measure the fission spectrum of neutrons. In our experiment, pulses from a Time to Amplitude Converter (TAC), similar to TPHC, are digitized. And this innovative idea of digitizing TAC pulses has been expected to give more precise measurement of the fission spectrum in lower energy region. By digitizing the TAC output, we should be able to measure the time of flight with considerably more accuracy than using a Multi-Channel Analyzer (MCA).

Our experiment consists mainly of two main detectors, a NaI gamma detector and a ^{6}Li neutron detector. As the name suggests, the conventional NaI gamma detector, which contains a NaI crystal, is sensitive only to gammas.

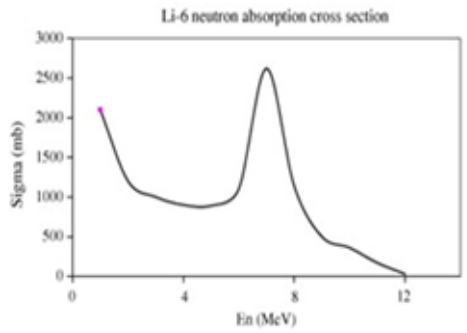

Figure 3: Neutron Absorption Cross Section of ^{6}Li

^{6}Li glass, on the other hand, is sensitive both to neutrons and gammas. However, its sensitivity to neutrons is very high compared to its sensitivity to gammas. The reason for using ^{6}Li in our experiment is its high cross section for low energy neutrons. In other words, it has a high probability of capturing low energy neutrons compared to the high energy ones, and low energy neutrons are exactly what we are interested in.

When ^{6}Li absorbs a neutron, it splits into an alpha and a tritium. As these charged particles lose energies in the glass, some of the energy is transferred to scintillator atoms. The ^{6}Li loaded glass contains small amounts of cesium as a scintillator. The scintillator atoms get excited to a higher energy state and then decay back down to the ground state, releasing a certain amount of energy in the form of a light photon. These photons hit the photocathode of a photomultiplier tube (PMT). The photocathode is coated with cesium so that it ejects electrons. These electrons are accelerated into the first dynode which

then eject more electrons. These electrons, in turn, hit another dynode, and so on, until one photon ejects millions of electrons from the last dynode, thus creating an electrical pulse. This pulse that is then used to measure the time of flight, and hence, the energy of the neutrons.

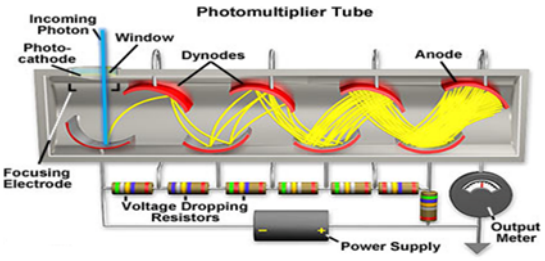

Figure 4: Diagram showing the electron multiplication process inside a PMT

As shown in Fig. 4, there are voltage dropping resistors in between dynodes. Because of these resistors, the potential in each dynode decreases as we go from left to the right. Since the energy gained by electrons is proportional to the voltage difference between the dynodes, electrons gain more energy as they move to the right. And hence, these energetic electrons eject more electrons from the dynodes on the right than the ones on the left. As a result, electron multiplication, and hence, generation of electric pulse, occurs.

A ^{60}Co gamma source is used for the calibration of the experimental setup for the time of flight experiment. ^{60}Co is a synthetic radioactive isotope of cobalt with a half-life of 5.27 years. It is produced artificially by neutron activation of the isotope ^{59}Co. ^{60}Co decays by beta decay to the stable isotope ^{60}Ni. The activated nickel nucleus emits two gamma rays with energies of 1.17 MeV and 1.33 MeV.

2 Preliminary Work

2.1 Construction of the Neutron Detector

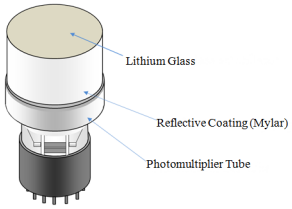

Figure 5: Diagram showing the sketch of Li glass neutron detector

First of all, I constructed a neutron detector with an Adit (Model ♯ B133DØ) PMT, 0.005" thick aluminized Mylar and a 2 mm thick, 5" diameter circular piece of Li glass. The diameter of Li glass is same as that of the PMT. The reason for using aluminized Mylar is its high surface reflectivity ($> 90\%$). Because of this, very few photons, emitted by the scintillation of Li glass, are lost on reflection by the Mylar.

To construct the detector, I placed a 6" high hollow cylindrical Mylar can around the PMT. Next, I glued the Li glass to a circular Mylar lid and taped the lid to the top of the Mylar cylinder, so that the non-glued face of the Li glass faced the PMT.

2.2 Optimum Distance Between Li glass and PMT

Before doing the time of flight experiment, the optimum distance between the ^{6}Li and PMT was calculated. If the ^{6}Li glass is too far from PMT, photons will be lost because of multiple reflections. On the other hand, if it is too close, the photons will hit only a certain area of the face of PMT. The response of the PMT is not uniform across the photocathode. A Monte Carlo program (written in MatLAB) gave the optimum distance of 6 cm. To find the optimum distance experimentally, the PMT was connected to a 1200 V power supply (the recommended optimum voltage) and the signal from the anode of the PMT was fed into a Ray Link signal digitizer. This detector was placed on the inside a Black Box (a box coated with black paint) to prevent the exposure of PMT to visible light photons. Exposure of PMT to visible light damages the tube.

Then, keeping the Li glass one meter from the ^{252}Cf source, data for different distances between the PMT and the Li glass were taken. The graph of the number of neutrons as a function of peak height was plotted. After this, the full width at half maximum (FWHM) of each distribution was measured. The formula to measure the FWHM of the distribution in percentage is as follows:

$$FWHM\,in\,\% = \frac{FWHM}{Position\,of\,the\,Peak} * 100\,\%$$

Since it is the ratio of FWHM to the position of the peak that matters, FWHM and the position of the peak can be measured in any arbitrary units. Examples of such units include volts, centimeters, etc.

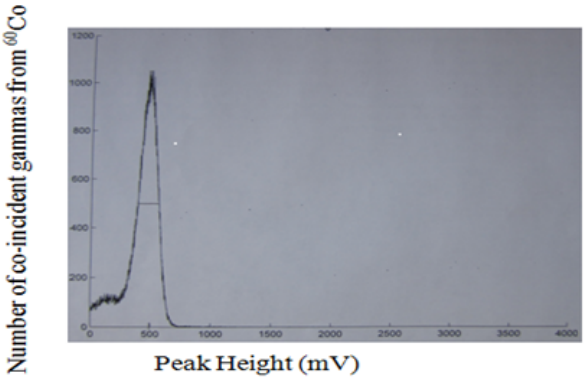

Figure 6: Peak Height distribution of the Li glass pulses, acquired from Ray Link Digitizer.

For this run, distance between the Li glass and PMT is 2.75". The FWHM=0.7 cm, and Position of the peak = 1.95 cm. Hence, FWHM=35.89%

After measuring the FWHM for different distances between the Li glass and the PMT, a parabolic least square fit, shown in Fig. 7, was obtained.

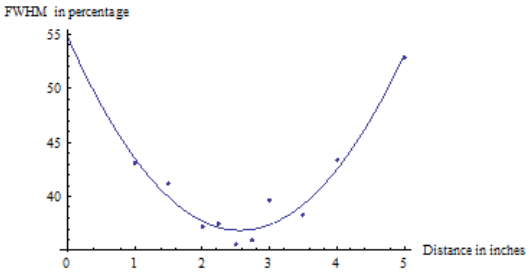

Figure 7: FWHM of the Peak Height Distribution (expressed in percentage) as a function of the distance between Li glass and PMT.

In Fig. 7, dots represent the actual data and the solid line represents the least square parabolic fit to the data.

From both the data and the fit, the optimum distance was found to be 2.5". This optimum distance is, to a high precision, in agreement with the distance predicted by Monte Carlo, which as mentioned above, was 6 cm. The purpose of minimizing FWHM of the peak height distribution was to eliminate gamma rays and get a good measurement of the number of neutrons.

3 Basic Setup and Working Mechanism

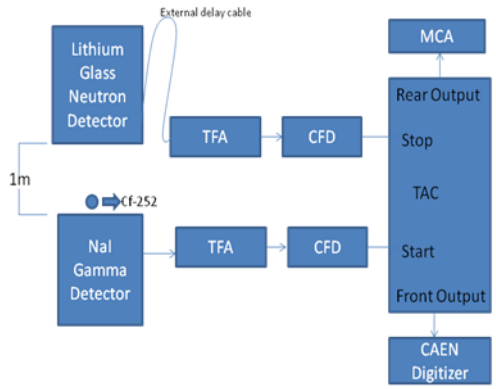

Figure 8: Schematic diagram of the experimental electronics to measure the time of flight of neutrons emitted from the spontaneous fission of ^{252}Cf neutron source.

This experiment consists of Ortec 474 Timing Filter Amplifiers (TFA), Ortec 583 Constant Fraction Discriminators (CFD), and a Time to Amplitude Converter (TAC). A Multi Channel Analyzer (MCA) is also used sometimes in parallel with the CAEN Digitizer.

As shown in Fig. 8, a ^{252}Cf neutron source is placed close to the NaI gamma detector and a meter farther from the neutron detector. As already described, a ^{252}Cf neutron source, after spontaneous fission, produces neutrons and gammas. One gamma thus emitted from a single fission event is absorbed by the NaI placed close to the ^{252}Cf.

On the other hand, a neutron, after traveling one meter, is absorbed by the neutron detector. Then, signals from these detectors are fed into corresponding TFAs where the pulses are amplified. After this, the output from each TFA is fed in to a CFD. Then, the output of the CFD from the NaI is fed into the stop input of the TAC and the output of the CFD from the neutron detector is fed in to the stop input of the TAC. An appropriate lower level threshold was set on the CFDs of both detectors to get rid of the accidentals or background pulses. As a result, only those signals whose amplitude exceed the lower level threshold will make it to the TAC.

This way, the TAC gives a square output signal for every Start input pulse that has a corresponding pulse in the Stop input of the TAC. In other words, every time there is a neutron or gamma in Li glass, corresponding to a gamma in NaI from the same fission event, the TAC gives a square output pulse. The amplitude of this output is directly proportional to the time difference between the start and stop input signal. Since the gamma time of flight is known, this difference determines precisely the neutron time of flight. Hence, the TAC gives the neutron time of flight, which then, with the given distance of 1m between the ^{252}Cf and Li detector, can be used to calculate the energy of neutrons and hence the fission spectrum.

The front panel output of the TAC is then fed into CAEN Digitizer and the rear panel output of the TAC is fed into MCA for further analysis.

4 Electronics

The electronic equipment involved in this experiment is described as follows:

4.1 Ortec 474 Timing Filter Amplifier (TFA)

Using the Course Gain and Fine Gain knobs in this amplifier, one can amplify the signal to the extent he/she wants. The Integration knob can be used to smooth signals.

4.2 Ortec 583 Constant Fraction Discriminator (CFD)

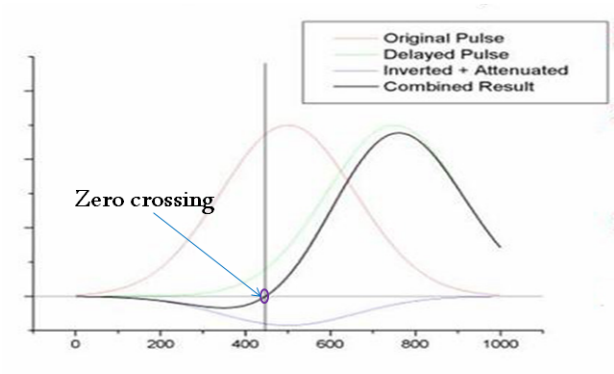

Figure 9: Diagram showing the function of CFD

As shown in Fig. 9, a CFD takes an input pulse and makes two copies of it. It delays one of the signals and then inverts and attenuates the other. After this, it adds up the two resultant pulses and produces a bipolar signal (dark black in the figure). The point in the time axis where the bipolar signal crosses the time axis is called the zero crossing point. It gives the time stamp to the original input pulse fed into it.

The extent, by which one of the copies of the input pulse is delayed, depends on the length of the CFD delay cable used. The length of the CFD delay depends on the nature of the pulse. In general, the CFD delay time is given by the following formula.

$$t_{CFD} = 1.1 * t_{rise} - 0.7\,ns$$

where t_{rise} denotes the rise time (time to go from 10% to 90% of the amplitude of the pulse) in nanoseconds (ns). The propagation delay of an RG-58 cable, as measured with a Digital Phosphor Oscilloscope, is 1.54 ns/ft. In other words, an electric pulse takes 1.54 ns to travel one foot of RG-58 cable. The value of propagation delay is also given by:

$$Delay = \sqrt{L * C}$$

where L is inductance and C is capacitance of the cable. For RG-58 cable, $L = 76.8\,nH/ft$, and $C = 21.2\,pF/ft$. So,

$$\text{Delay} = \sqrt{76.8 * 10^{-9} * 31.2 * 10^{-12}} = 1.55\,ns/ft$$

This agreed very well with our measured value of $1.54\,ns/ft$.

Then, the length of the CFD delay cable is given by $\frac{t_{CFD}}{1.54\,ns/ft}$, where t_{CFD}, as mentioned above, is in ns. This formula, in general, gives a crude CFD delay cable length. One needs to experimentally optimize the length of the CFD delay cable. One thing to keep in mind is that CFDs only take negative input signals.

The CFD can be run in different modes. Some of them are described below.

4.2.1 Diff/Int

In differential mode, the CFD allows only those pulses whose amplitude lie between the Lower Level Threshold and Upper Level Threshold to go through. Both the Lower Level and Upper Level thresholds can be set in the CFD. In Int mode, however, the CFD allows only those pulses whose amplitude exceed the Lower Level Threshold to go through. In general, Diff mode is preferred over Int mode as Diff mode helps avoid saturated pulses.

4.2.2 CF/SRT

In Constant Fraction (CF) mode, the CFD produces bipolar signals and gives a zero crossing point as shown in Fig. 9. As the name itself implies, in Slow Rise Time reject (SRT) mode, the CFD rejects pulses with slow rise time.

Quad CFDs were also used hoping to get better results. However, the operation of Quad CFDs, unlike the Ortec 583, was based on the time for the pulse to go from 20% to 100% of the amplitude. Since this time is less consistent compared to the rise time, Quad CFDs were not used.

4.3 Ortec 567 Time to Amplitude Converter (TAC)/ Single Channel Analyzer (SCA)

The TAC has a large capacitor that charges linearly as the voltage builds up. It gives a square output signal whose amplitude is directly proportional to the time difference between the start and stop input pulse. With our 12 bit digitizer system, it is possible to measure time up to 0.1 ns whereas if we measure time directly with a digitizer, we can measure time only in steps of 4 ns. The TAC window can be set by using the knobs Range(ns) and Multiplier. Throughout this experiment, the TAC window was set at 500 ns (50 ns in Range and 10 in Multiplier), because it covered the range of energy of neutrons of interest for the experiment.

5 Fission Spectrum Experiment

5.1 Minimizing Timing Resolution with ^{60}Co

Before working on the time-of-flight experiment with ^{252}Cf, the timing resolution of the experimental setup was minimized using coincident gammas from ^{60}Co. The experimental setup for this purpose was almost the same as that for the fission spectrum experiment (shown in Fig. 8), except that the ^{252}Cf source was replaced with ^{60}Co, which was then placed in between the two detectors.

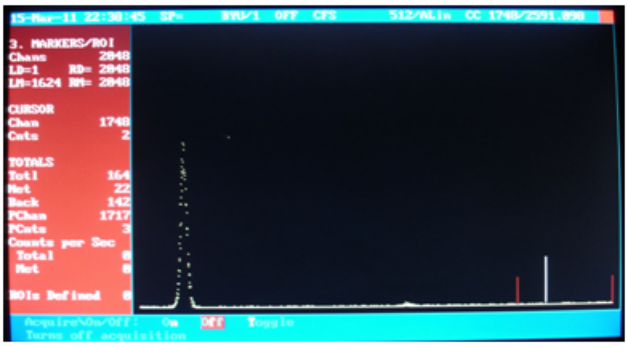

Figure 10: MCA window displaying a run for timing resolution experiment.

In Fig. 10, the horizontal axis in this graph is voltage and the vertical axis is Number of coincident gammas. The rear panel output of the the TAC was fed into the MCA for this run. The output of the MCA ranges from 0 to 10 V (the horizontal scale in Fig. 10). As already mentioned above, the TAC window was set at 500 ns. So, the horizontal scale in voltage can easily be converted into ns. Typically, 1V translates to 50 ns time difference between the start and stop pulses. Since the time difference between coincident gammas (start and stop input in this run) is zero most of the time, an external delay cable (as shown in Fig. 8) was added to the stop pulse (which for this experiment is the ^{6}Li detector) to see the entire peak. The external delay cable used for the run shown in Fig. 10 is 40 ft.

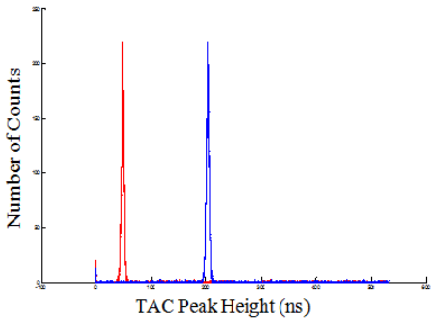

Figure 11: Calibration of the experimental setup for timing resolution with coincident gammas from ^{60}Co.

Fig.11 shows the peak height distribution of TAC pulses for two different external delay cables, 43.12 ns (28ft) and 204.82 ns (133ft). After this calibration, the FWHM of the peaks was measured.

The FWHM, in this case, is a function of many variables. These variables include course gain, fine gain, and integration in the TFA, lower level threshold and CFD delay cable lengths in the CFD, appropriate use of terminators, etc. To minimize timing resolution, each variable was changed keeping all other variables constant, and FWHM was measured by calibrating the setup as shown in Fig. 11.

Since there were many variables associated with the FWHM, minimizing timing resolution took a significant amount of time. The minimum timing resolution obtained after optimizing all these variables was 1.5 ± 0.1 ns .

5.2 Procedure for the Timing Resolution Experiment

5.2.1 Configuration

During this experiment (and the area distribution experiment that will be discussed in next two sections), an ORTEC base was used on the Adit PMT of the ^{6}Li neutron detector. The signal from the anode of the ORTEC base was fed into the TFA while the dynode was terminated with a 50Ω terminator to prevent the reflection of the signal. The NaI detector, on the other hand, used a Canberra base. Its dynode, however, need not be terminated. An optimum voltage of 1200V was supplied to the NaI and the Adit PMT, and 2000V to the Hamamatsu tubes. Hamamatsu tubes have very fast rise time compared to Adit PMT, and hence the timing resolution with Hamamatsu tubes was expected to be better. However, the pulses produced by the Hamamatsu tubes were so jittery that even the pulses, which were smoothed out using the Integrate knob on the TFA, did not look as smooth as the raw pulses from Adit PMT. Hence, the Hamamatsu tubes were not used later.

The configuration for the optimum timing resolution (1.5 ns) is as follows:

a) NaI: TFA: Course Gain = 6; Fine Gain=4; Int=0; Diff=0; Non-Inv (Non-Inv/Inv); CFD: Selected toggle switches :- CF (CF/SRT), Int (Int/Diff); Lower Level Threshold = -350 mV; Upper Level Threshold = -5V; CFD delay cable = 50ft; Gain and focus in the Canberra base were set at their maximum value. Also. at the input of the TFA, a 100Ω resistor was always placed in parallel with the incoming anode pulse of PMT to match the impedance of the TFA.

b) ^{6}Li detector: TFA: Course Gain = 6; Fine Gain=4; Int=0; Diff=0; Non-Inv (Non-Inv/Inv);100Ω resistor in parallel with the NaI anode signal going into the TFA for the reason described above. CFD: Selected toggle switches :- CF (CF/SRT), Int (Int/Diff); Lower Level Threshold = -100mV; Upper Level Threshold = -5V; CFD delay cable = 10ft; The dynode of the Ortec base with ^{6}Li detector was terminated with a 50Ω terminator.

c) TAC: TAC window = 500 ns; Selected toggle switches :- Int (Int/Ext), Anti (Anti/Coinc), Anti (Anti/Coinc), OUT (TAC inhibit/OUT), a 6dB attenuator in series with a 20dB attenuator at the front panel output of the TAC going into the CAEN digitizer.

Setting the toggle switch at OUT (instead of TAC inhibit) ignores the SCA timing window which can be set by using the SCA Lower Level (T) and SCA window (ΔT) knobs. Setting the toggle switch at TAC inhibit allows only those pulses which lie within the SCA window to go through. But since the TAC window (set at 500 ns) was required to not be interfered by the SCA window, the toggle switch was set to the OUT position.

The two detectors were placed 26" apart and the ^{60}Co was placed in between. Two runs, each with a different external delay cable (as shown in Fig. 11) added to the ^{6}Li, were taken. It was then calibrated (as shown in Fig. 11) and the timing resolution was measured. The external delay cable was added to the ^{6}Li to shift the peak to the middle of the window. The rest of the cable lengths, between the two branches, were kept the same.

However, the external delay cable should never be added between the ^{6}Li CFD output and the stop input of the TAC. The CFD gives a tiny (4 ns wide) negative timing output pulses that are fed into the input of the TAC. However, the TAC demands the minimum threshold of these CFD timing output pulses to be around -1V. Now, if a long external delay cable is added in between the CFD timing output and input of the TAC, the cable will attenuate the timing signal coming out of the CFD, and the low amplitude pulses may not meet the -1V minimum threshold requirement of the TAC. As a result, the TAC will not see any input pulses and hence, will not produce any output pulses. This is exactly what happened with this timing experiment. The TAC stopped giving output pulses for any external delay above 150ft added between the CFD timing output and the TAC input. But when the external delay was added between the anode of the NaI and its TFA, the TAC gave output pulses.

Another important thing to keep in mind while feeding the signal from the TAC to the CAEN digitizer is to use appropriate attenuation at the output of the TAC. The TAC output ranges from 0 to 10V while that of the CAEN ranges from 0 to 1V. Since 20dB attenuates the voltage by a factor of 10, using a 20dB attenuator at the output of the TAC (going into the CAEN) should be good enough. However, an additional 6dB attenuator, which attenuates voltage by a factor of 2, was used in series with the 20dB attenuator. As a result, the signals are attenuated by a factor of 20. Hence, the pulses in the CAEN never exceed 500mV. And since the TAC window is set at 500ns, 1 mV in the CAEN corresponds to 1 ns. And this makes the conversion of mV to ns very convenient. This is why an additional 6dB attenuator was used in series with the 20dB attenuator, though 20dB is good enough to prevent the saturation of signals in the CAEN.

One crucial thing to keep in mind while using the CFD delay cable is to make sure that the connections in the CFD delay cable (if connected with barrels and connectors) are good. If there is a connection problem in the cable (or if the cable is bad), the CFD, would in general be expected to not give any output pulse. However, this is not the case. The CFD still gives an output pulse. This output pulse comes approximately 800 ns after the CFD input pulse. In other words, the inherent delay in the CFD output pulse relative to the input pulse, if the CFD delay cable is bad (or if there is no CFD delay cable), is 800 ns. If this problem is not properly addressed, then this will produce misleading data.

5.2.2 Data Acquisition

The signal from CAEN is fed into Good Controller (GC) for data acquisition. The Peek button in GC was clicked couple of times to check to see whether or not DC offset was set to zero. If not, the DC offset was adjusted and set to zero. An appropriate positive (because TAC output pulses are positive) lower level threshold was set. Moreover, a Minimum Pulse Width of 1000 ns (as TAC pulses are very wide) was specified to get rid of the noise. Zero Level Encoding (ZLE) parameters were left at their default positions as they were not required for TAC peak height measurement. Rising (Falling/Rising) and Header (Header/No Header) was chosen.

A time window of 1000 samples (4 μs) was chosen to capture the entire pulse. A post trigger was set at around 70% of the window. After clicking the Start Acquisition button, GC starts to record the data. While the data acquisition is in process, one can click the Plot button at the bottom of the pulse window and look at the pulses. However, to see the pulses in the window, the Disk Buffer size has to be set to an appropriate value. An easier way to do it is look at the bottom left of GC where numbers like 382KB/s are displayed. Then, if the value of the Disk Buffer Size is set around that value (say 350KB or 400KB), then the pulses can be seen more frequently. However, if the value for the Disk Buffer Size is set at a very large value (say 10000KB), then the GC will wait until it has acquired 10000KB of data to display one pulse. Hence, to see the pulses by clicking Plot button while the data acquisition is in process, one has to choose an appropriate value for Disk Buffer Size. However, if one does not want to look at the pulses, Disk Buffer Size can be assigned any value as it does not affect the data acquired. For the timing resolution experiment, a Disk Buffer Size of 1KB was chosen since the rate of the TAC pulse with the weak ^{252}Cf source is really low (around 10,000 pulses in every 24 hours). One can choose to stop the acquisition after running the program for certain amount of time or after acquiring certain number of counts, both of which can be specified in GC. For this timing resolution experiment, GC was set to stop after recording 10,000 counts. This facilitates the ^{252}Cf source to be taken away for other experiments without stopping the acquisition. The rest of the settings in GC were kept at their default position. To avoid resetting all these variables once GC is closed, each such configuration (with all the variables properly specified) can be saved and loaded once GC is opened, for convenience.

5.2.3 Analysis

The data acquired in GC were analyzed in MatLAB. First of all, the file created by GC was loaded into a MatLAB file. Then, the maximum of each TAC pulse was located. Points, corresponding to the half of the maximum on either side of the maximum, were then located. Then, the average of those two point numbers was rounded to the nearest integer. Next, we went 100 points on either side of the average point and took the mean of the value of the peak between the two new points. For example, if the average point is 2000, then mean of the value of pulse between points 1900 and 2100 was taken to find the peak height of the TAC pulse. Since the TAC pulse is not always flat on top, taking average is a better way of finding the peak height rather than just taking the maximum of the pulse. Then, a histogram of peak distribution (Fig. 11 for example) was plotted.

5.3 Area Distribution of ^{6}Li Pulses with the ^{252}Cf Neutron Source

After minimizing the timing resolution, we were ready to work on the fission spectrum of ^{252}Cf. However, when the ^{252}Cf source was placed next to NaI, and about a meter farther from the ^{6}Li detector (as depicted in Fig. 8), no neutron bump was seen on the time-of-flight distribution of the TAC output. To make sure that the neutron detector was seeing neutrons, we plotted the area histogram of the pulses from TFA output from the NaI detector. Since the output of the TFA goes up to 10V, a 20dB attenuator was connected to the output of the TFA going into the CAEN, to make sure that the voltage in CAEN does not go above 1V.

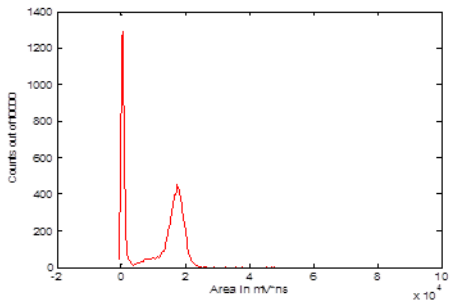

Figure 12: Area histogram of ^{6}Li pulses

Fig. 12 shows the area distribution of Li glass pulses coming out of the TFA (with a 20dB attenuation at TFA output.For this particular run, a few blocks of wax were placed in between the ^{252}Cf and the ^{6}Li detector. The gamma peak (to the left) is followed by a neutron bump. It is apparent from Fig. 12 that the area of the neutron peak are greater than that of the gamma peak.

5.4 NaI Spectrum of ^{60}Co

Though neutrons were seen in the area distribution of ^{6}Li pulses with the ^{252}Cf source, they were still not being seen in the time of flight experiment with the ^{252}Cf source. So, to make sure that the NaI detector was not broken, the NaI spectrum with ^{60}Co was taken. However, when the lower level threshold, used in CFD for time of flight experiment (in which no neutrons were seen), was used (in GC) to acquire the NaI spectrum, the spectrum acquired did not look like the well-known spectrum of NaI. So, the lower level threshold of NaI (in CAEN Digitizer) was adjusted until the expected spectrum was seen.

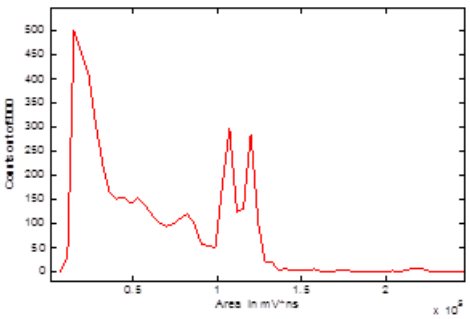

Figure 13: Area histogram of the NaI pulses with ^{60}Co.

NaI spectrum of ^{60}Co, shown in Fig. 13, matches very well with the well-known NaI spectrum of ^{60}Co.

5.5 Procedure for Area Distribution Measurement

5.5.1 Configuration

To acquire the area distribution (both Fig. 12 and 13) data, a signal from the anode of the PMT was fed into the TFA. A 100 Ω resistor was connected in parallel with the anode signal at the TFA input to match the impedance. A Course Gain of 6 and a Fine Gain of 4 were set in the TFA. Both the Diff and Int. knobs in the TFA were set to zero. Since the output of the TFA goes up to 10V and the CAEN can only take up to 1V, an attenuation of a factor of 10 (a 20dB attenuator) was connected at the TFA output going into the CAEN.

5.5.2 Data Acquisition

Different settings were chosen in Good Controller (GC) after the signal from CAEN was fed into a computer. A lot of settings and procedures are very similar to those of the timing resolution experiment. First, the DC offset in GC was set to zero. An appropriate negative (because anode pulses are negative) lower level threshold and a Minimum Pulse Width of 100 ns was chosen to get rid of the noise. Zero Level Encoding (ZLE) parameters were kept at their default values as they were not required for area distribution measurement. Falling (Falling/Rising) and Header (Header/No Header) were chosen. A Disk Buffer Size of 35KB was chosen. A time window of 1000 samples (4 μs) was chosen to capture and the post trigger was set at around 70% of the window. Out of the two options of choosing to stop the acquisition after running GC for certain amount of time or after acquiring certain number of counts, counting was preferred. GC was set to stop acquisition after acquiring 10,000 counts. The rest of the settings in GC were left at their default position. To avoid resetting all these variables once GC is closed, each such configuration (with all the variables properly specified) was saved.

5.5.3 Analysis

The data acquired in GC is analyzed in MatLAB. First of all, the file created by GC was loaded into a MatLAB. Then, the negative pulse in the file was inverted to make it positive as it makes the analysis easier. Next, the maximum of the positive pulse was located and the points corresponding to a third of the maximum on each side of the peak of the pulse were located. Then, we went back 30 channels on either side of the pulse. The area of the pulse between these points was determined. For example one third of the maximum occur at points 300 and 700. Then, pulse between points 270 to 730 was integrated to calculate the area. After this step, an area histogram (Fig. 12 and 13 for example) was plotted.

6 Time-of-Flight Experiment with the ^{252}Cf Neutron Source

To do the time-of-flight experiment, appropriate thresholds were set on the CFDs of the NaI and the ^{6}Li detector. First, NaI anode pulses were fed into a TFA. Then, the TFA output was teed off and one of the output was fed into the oscilloscope while the other was fed into a CFD. Voltage corresponding to the maximum peak height of anode pulses in the oscilloscope was noted. Let us, for convenience, call it maximum voltage. Next, dynode pulses from the NaI was fed in to another TFA (let's call it dynode TFA) and the output from this TFA was fed into the oscilloscope. Then, the output of the CFD to which NaI anode pulses were fed, was used to trigger the output of the dynode TFA in the oscilloscope. The Lower Level Threshold in the CFD was then increased until all the dynode pulses exceeded the maximum voltage. This voltage is precisely the lower level threshold we wanted to set on the CFD. For this experiment, this voltage was experimentally found to be 1.0V.

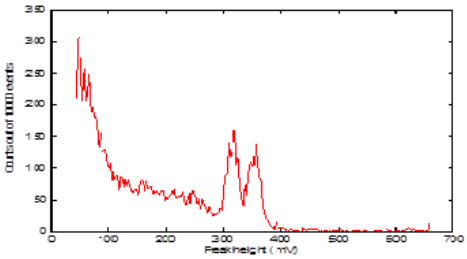

Figure 14: NaI peak height distribution of ^{60}Co

Fig. 14 shows the peak height distribution of ^{60}Co (with three 6dB attenuators connected in series at the TFA output going into the CAEN digitizer). The maximum voltage, as can be seen in Fig. 14, occurs at around 400mV. This voltage, because of the use of three 6dB (attenuates the voltage by a factor of 2) attenuators, translates to 2.4V. We wanted to set the threshold to half of this which is 1.2V. This is in agreement with 1V that we got using the method described above.

Now that the thresholds in both the CFDs were appropriately chosen, we were ready to make the time-of-flight measurements.

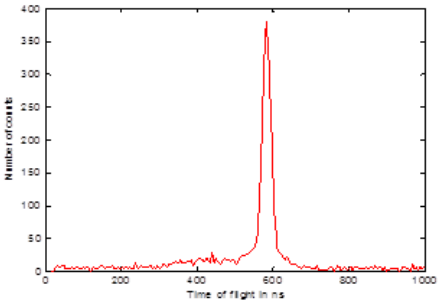

Figure 15: Early time-of-flight run after setting appropriate thresholds in CFDs.

We can see a small neutron bump to the left of the huge gamma peak. Since the ^{6}Li is fed into the start input of the TAC and the NaI to the stop input (with an external delay in NaI), high energy neutrons are close to the gamma peak and low energy neutrons are far on the left.

Since we were seeing too many gammas compared to neutrons, we decided to look only at those TAC pulses which had, in the corresponding ^{6}Li pulse a neutron instead of gammas. So, we fed the TAC pulse into channel 2 of the CAEN digitizer and the output of the dynode TFA (another TFA to which the dynode of ^{6}Li was fed) in to channel 2 of the digitizer. The settings in this dynode TFA were same as that of the TFA going in to the TAC. Then, in GC, we first set the DC offset of both channels to zero. We triggered on channel 3 and enabled both channel 2 and channel 3. The settings for the TAC in good controller were the same as before except one. The TAC pulse was observed in

oscilloscope to come about 2 μs after the ^{6}Li dynode pulse. Moreover, the TAC pulse itself is about 2 μs wide. As a result, the usual 1000 samples (4 μs) setting in GC was not wide enough to capture both the TAC and the ^{6}Li dynode pulses in GC. Hence, we had to change it to 4000 samples (16 μs) to capture both the TAC and the ^{6}Li dynode pulse. The rest of the settings in GC were set at values same as that for the timing resolution experiment.

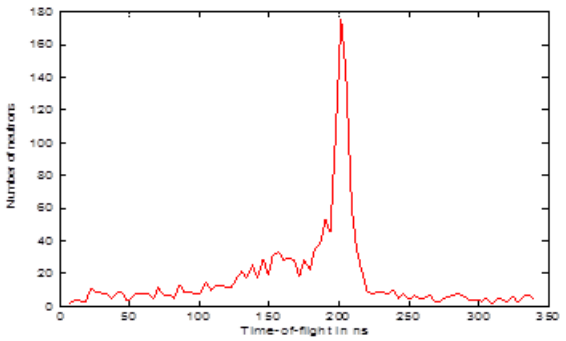

Figure 16: Time-of-flight distribution of neutrons after setting restrictions on the area histogram of the ^{6}Li pulses

Since the resolution of the area distribution is much better than that of peak height distribution, we set a certain restriction in the area distribution to capture the neutron bump (shown in Fig. 12) and only look at the TAC pulses with corresponding ^{6}Li pulses within the neutron bump. The neutron bump looked more prominent after setting these restrictions in the ^{6}Li pulses.

7 Rate of Neutrons vs Kinetic Energy

After the acquisition of the time of flight information, the rate of neutrons as a function of kinetic energy was calculated. As opposed to the uniform time bins, the following kinetic energy bins in MeV were used.

$$0.1, 0.125, 0.175, 0.25, 0.35, 0.45, 0.55, 0.7, 0.9, 1.25, 1.75, 2.5$$

Kinetic energy was calculated from time of flight information using the following relativistic formula.

$$KE = (\gamma - 1) m\, c^2$$

where $\gamma = \frac{1}{\sqrt{1-\frac{v^2}{c^2}}}$ and $v = \frac{d}{t}$.
Here, c (speed of light) $= 3 * 10^8 \frac{m}{s}$,
$m\, c^2$ (rest energy of a neutron) $= 940$ MeV,
d (distance between the ^{252}Cf source and ^{6}Li glass) $= 80$ cm,
and t is the time of flight of the neutron. The rate of neutrons is then given by

$$S_i = \frac{N_i}{E_i \frac{\Omega}{4\pi}}$$

where Ω is the solid angle and N_i is the number of neutrons in the kinetic energy bin KE_i. N_i is obtained from the histogram of KE. Moreover, E_i is given by

$$E_i = 1 - e^{\frac{A * \Delta x * \rho * \sigma_i}{MW}}$$

where
A (Avogrado's number)= $\frac{6.022 * 10^{23}}{mol}$,
Δx (thickness of ^{6}Li glass)=0.2 cm,
ρ (density of ^{6}Li)=1.56 $\frac{g}{cm^3}$,
σ_i = cross section of ^{6}Li at kinetic energy KE_i,
MW (molecular weight of ^{6}Li)= 6.941 $\frac{g}{mol}$

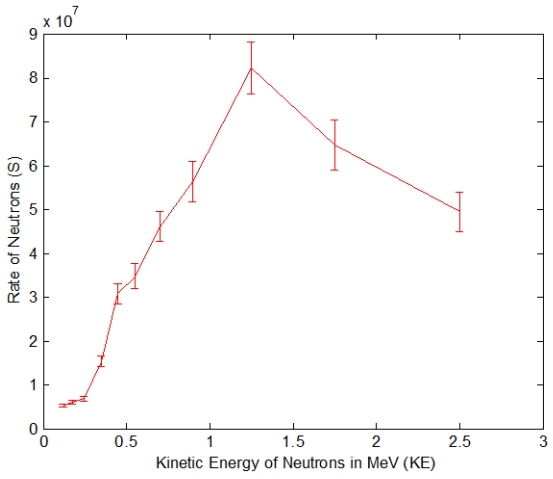

Figure 17: Rate of neutrons as a function of their kinetic energies

Figure 17 matches reasonably well with the neutron spectrum of spontaneous fission of ^{252}Cf. The spectrum peaks at about 1.25 MeV and then starts to drop off above 1.25 MeV. We have few counts on the very low energy portion of the spectrum. The neutron cross section of ^{6}Li at various kinetic energies were taken from reference [7]. The uncertainties in the graph are based on counting statics, $\Delta N_i = \sqrt{N_i}$ where N_i is read off of the histogram of kinetic energy, as explained above.

8 Conclusion

Using a NaI gamma detector and a ^{6}Li glass neutron detector, we attempted to measure the fission spectrum of neutrons with kinetic energies less than 1 MeV emitted from the spontaneous fission of ^{252}Cf to a greater precision than before. After making sure the NaI spectrum ^{6}Li spectrum look like the way they are supposed to, coincident gammas were used to calibrate the experimental setup consisting of electric units such as TFA, CFD, MCA and TAC. Then, the kinetic energy and hence the rate of neutrons were measured using the time of flight techniques and the geometry of the detectors. The measured neutron spectrum is consistent with the known spectrum.

Our measurements, however, was only a preliminary measurement that established techniques that could be used in a careful experiment that will be done later. We could have measured the fission spectrum to a greater precision using this innovative idea of digitizing TAC pulse if we could perform the experiment without room return neutrons. Since the experiment was conducted inside a lab where the neutron detector was prone to the neutrons reflected from the floor, wall and ceiling of the lab, avoiding such room return neutrons will lead to more precise measurement of the energy of neutron. To do this, the experiment will be performed on the platform of a scissor lift. Moreover, the statistical uncertainty of the data is too large. It took about three days to get data using the ^{252}Cf source we have. So, using a stronger source will increase the rate of data acquisition and expedite the progress of the experiment.

9 BIBLIOGRAPHY

1. Figure 1:
http://www.chemicool.com/elements/uranium.html
2. Figure 2:
Chichester,D.L., Johnson,J.T., & Seabury,E.H. (2011).Fast-neutron spectrometry using a ^{3}He ionization chamber and digital pulse shape analysis. *Applied Radiation and Isotopes, 70*, 1457-1463.
Retrieved from
http://www.sciencedirect.com/science/article/pii/S0969804311006828
3. Figure 3:
Faghihi F., Havasi H., & Amin-Mozfari M. (2007). Plutonium-239 production rate study using a typical fusion reactor. *Annals of Nuclear Energy, 35*, 759-766.
Retrieved from
http://www.sciencedirect.com/science/article/pii/S0306454907002733
4. Figure 4:
http://digitalimagingu.com/articles/photomultipliers.html
5. Figure 9:
http://www1.chem.leeds.ac.uk/PICNIC/members/photek1.htm
6. Meadows J.W. (1967). ^{252}*Cf Fission Neutron Spectrum from 0.003 to 15.0 MeV*, 157.
7. Knoll, G.F., (2000). *Radiation Detection and Measurement* (3rd ed.). Hoboken, NJ: John Wiley & Sons, Inc.